View Article Online / Journal Homepage / Table of Contents for this issue

Double and triple stranded mesocates containing the bis(bidentate) bridging ligand 1,3-bis(pyridine-2-carboxamide)benzene. Structure, properties and DNA interaction†

M[a]Angeles Palacios,[a] Antonio Rodríguez-Diéguez,[a] Angelo Sironi,[b] Juan Manuel Herrera,[a] Antonio J. Mota,[a] Virtudes Moreno,[c] Joan Cano[d] and Enrique Colacio*[a]

Received (in Montpellier, France) 17th March 2009, Accepted 9th June 2009
First published as an Advance Article on the web 13th July 2009
DOI: 10.1039/b905330a

Published on 13 July 2009 on http://pubs.rsc.org | doi:10.1039/B905330A
Downloaded by University of Belgrade on 02 January 2013

The double stranded Cu^{II}_2 metallacyclic complex of formula $[Mn(hfac)_2(H_2O)_2][Cu_2(mbpb)_2(CH_3CN)_2]$ (**1**) and the triple stranded Ni^{II}_2, Zn^{II}_2 and Co^{III}_2 metallacyclic complexes of formula $[M_2(Hmbpb)_3]X{\cdot}nH_2O$ (M = Zn^{II}, X = NO_3^- (**2**), n = 17; M = Ni^{II}, and X = ClO_4^- (**3**), n = 15) and $[Co_2(mbpb)_3]{\cdot}19H_2O$ (**4**) (H_2mbpb is the bisbidentate dinucleating bridging ligand, 1,3-bis(pyridine-2-carboxamide)benzene) have been prepared and structurally characterised. Their X-ray structures show that inside the dinuclear molecules metal ions are bridged by either fully or semideprotonated bisbidentate ligands, which are coordinated through the pyridine and amidato nitrogen donor atoms. In **1**, the neutral metallamacrocycle dinuclear entities $[Cu_2(mbpb)_2(CH_3CN)_2]$ and the $[Mn(hfac)_2(H_2O)_2]$ molecules are connected by hydrogen bonds to afford a 1D system. These intermolecular interactions overcome the expected intradinuclear weak ferromagnetic interaction leading to an overall weak antiferromagnetic interaction. The Ni_2 complex exhibit ferromagnetic coupling between the metal ions through the bridging ligand with J_{Ni-Ni} = 3.1 cm^{-1}. DFT calculations were performed to estimate the value of the exchange magnetic coupling inside the dinuclear unit in **1** and to confirm that the spin polarisation mechanism is responsible for the ferromagnetic coupling. AFM studies show that the Zn^{II}_2 and Ni^{II}_2 cationic complexes interact with pBR322 DNA producing supercoiled forms in higher extension as well as kinks and cross linking.

Introduction

During the past two decades, a great deal of attention has been paid to double and triple stranded dinuclear helicates complexes in connection with the self assembly of metallo-supramolecular architectures. These systems, which are often considered as the simplest and most fundamental of supramolecular structures, have been used as simple models to study the elemental principles that direct the self-assembly of supramolecular architectures promoted by metal coordination. Helicates are also of interest because of their involvement in new areas of research such as anion sensors, bioinorganic chemistry, luminescence, magnetism, chirality, guest recognition, *etc*.[1] Moreover, it has been shown recently that relatively simple dinuclear cationic helicates strongly bind to DNA and cause remarkable and unprecedented effects on DNA structure.[2] Among metallacycles, those exhibiting magnetic properties have been studied in connection with stepwise spin-crossover properties[3] and ferromagnetic coupling through a spin polarisation mechanism.[4] The study of helicates has shown that the specificity of the self-assembly of supramolecular structures depends on the symmetry of the molecular components: the stereoelectronic preference of the metal ions and the disposition of the binding sites in the ligand.[1] Therefore, the appropriate choice of the bridging ligands and metal ions are crucial for the deliberate design of double and triple helicates. If the achiral ligands are twisted around the metal ions, homochiral (Δ or Λ) helicates are formed. The side-by-side coordination of the ligands, however, results in achiral *meso*-helicates (mesocates), in which metal centers exhibit opposite chirality (Δ and Λ).

We report here on the syntheses, structures, magnetic properties and DFT studies of the double stranded Cu^{II}_2 metallacyclic mesocate complex of formula $[Mn(hfac)_2(H_2O)_2][Cu_2(mbpb)_2(CH_3CN)_2]$ (**1**) and the triple stranded Ni^{II}_2, Zn^{II}_2 and Co^{III}_2 mesocates of formula $[M_2(Hmbpb)_3]X{\cdot}nH_2O$ (M = Zn^{II}, X = NO_3^- (**2**), n = 17; M = Ni^{II}, X = ClO_4^- (**3**), n = 15) and $[Co_2(mbpb)_3]{\cdot}19H_2O$ (**4**) (H_2mbpb is the bisbidentate dinucleating bridging ligand, 1,3-bis(pyridine-2-carboxamide)benzene, Scheme 1). As the

[a] *Departamento de Química Inorgánica, Universidad de Granada, 18071, Granada, Spain. E-mail: ecolacio@ugr.es; Tel: 0034958243236*
[b] *Dipartimento di Chimica Strutturale e Stereochimica Inorganica, CNR-ISTM, Università di Milano, via Venezian 21, 20133-Milano, Italy*
[c] *Departament de Química Inorgánica, Universitat de Barcelona, av. Diagonal, 647, 0.8028-Barcelona, Spain*
[d] *Departament de Química Inorgànica and Centre de Recerca en Química Teórica, Institució Catalana de Recerca i Estudis Avançats (ICREA), Universitat de Barcelona, 08028-Barcelona, Spain*
† CCDC reference numbers 723672, 723673, 723674 and 721059. For crystallographic data in CIF or other electronic format see DOI: 10.1039/b905330a

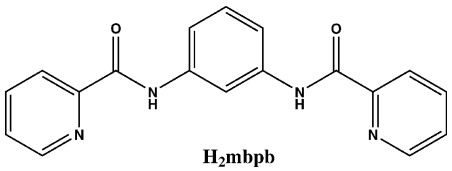

H_2mbpb

Scheme 1

ligand possesses a mirror plane, it is predisposed to form achiral mesocates. In addition we have investigated the interaction between the cationic helicates **2** and **3** and DNA with the aim of knowing whether or not the magnetic properties of the helicates (diamagnetic or paramagnetic) affect such an interaction.

Experimental

General

All analytical reagents were purchased from commercial sources and used without further purification. The ligand H_2mbpb was prepared according to a previously described procedure.[5] pBR322 plasmid DNA was obtained from Boehringer–Mannheim (Mannheim, Germany). pBR322 plasmid DNA is 4361 base pairs and contains over 60% double-strand closed circular form I. HEPES (*N*-2-hydroxyethylpiperazine-*N*′-2-ethanesulfonic acid) was obtained from ICN (Madrid).

Synthesis of the complexes

$[Mn(hfac)_2(H_2O)_2][Cu_2(mbpb)_2(CH_3CN)_2]$ (1). A solution of $[Mn(hfac)_2(H_2O)_2]$ (0.192 g, 0.41 mmol) in 10 mL of CH_3Cl was added dropwise with continuous stirring to a suspension of 0.05 g (0.063 mmol) of the complex $[Cu_2(mbpb)_2]\cdot 2H_2O$ (which was obtained as a black powder from the reaction of the ligand with $Cu(OAc)_2\cdot H_2O$ in methanol using a 1 : 1 molar ratio) in 10 mL of $CHCl_3$ and the mixture was further stirred for 30 min. A green powder was obtained after slow evaporation of the resulting green solution at room temperature. This solid was recrystallised from acetonitrile and the solution kept at room temperature for several days afforded dark green crystals suitable for X-ray crystallography. Yield: 30%. Anal. Calc. for $C_{50}H_{36}N_{10}O_{10}F_{12}Cu_2Mn$: C, 44.59.47; H, 2.69; N, 10.40. Found: C, 44.32; H, 2.38; N, 10.60%. IR (KBr, cm^{-1}): 3414, ν(OH); 1620, ν(C═O); 1592, ν(C═C); 1569, ν(CN); 1257, 1203, 1143, ν(C–F).

$[Zn_2(Hmbpb)_3]NO_3\cdot 17H_2O$ (2). NaOH (40 mg, 1 mmol) and $Zn(NO_3)_2\cdot 6H_2O$ (0.098 g, 0.333 mmol) were successively added to a solution of the H_2mbpb ligand (0159 g, 0.5 mmol) in 20 mL of hot methanol while stirring and the mixture refluxed for 2 h. The colorless resulting solution was allowed to stand at room temperature for several days, whereupon X-ray quality prism crystals were obtained. They were filtered and air dried. Yield: 20%. Anal. Calc. for $C_{54}H_{73}N_{13}O_{26}Zn_2$: C, 45.27; H, 4.24; N, 12.04. Found: C, 44.90; H, 4.67; N, 12.37%. IR (KBr, cm^{-1}): 3405, ν(OH); 1608, ν(C═O); 1580, ν(C═C); 1560 ν(C–N); 1384, $\nu(NO_3)$.

$[Ni_2(Hmbpb)_3]ClO_4\cdot 15H_2O$ (3). This compound was prepared by following the same method as for **2** but using $Ni(ClO_4)_2\cdot 2H_2O$ (0.123 g, 0.333 mmol) instead of $Zn(NO_3)_2\cdot 6H_2O$. The resulting brown-greenish solution was allowed to stand at room temperature for several days affording X-ray quality crystals of **3**, which were filtered off and air dried. Yield: 30%. Anal. Calc. for $C_{54}H_{69}N_{12}O_{25}Ni_2Cl$: C, 38.91; H, 4.17; N, 10.08. Found: C, 38.79; H, 3.97; N, 10.35%. IR (KBr, cm^{-1}): 3420, ν(OH); 1608, ν(C═O); 1580, ν(C═C); 1560 ν(C–N); 1094 ν(Cl–O).

$[Co_2(mbpb)_3]\cdot 19H_2O$ (4). This compound was prepared by following the same method as for **2** but using $Co(NO_3)_2\cdot 6H_2O$ (0.097 g, 0.333 mmol) as the metallic salt. The resulting red solution, kept at room temperature for several days, afforded red crystals suitable for X-ray analysis. Yield: 15%. Anal. Calc. for $C_{54}H_{74}N_{12}O_{25}Co_2$: C, 46.03; H, 5.29; N, 11.93. Found: C, 46.38; H, 4.95; N, 11.72%. IR (KBr, cm^{-1}): 3787, ν(OH); 1625, ν(C═O); 1595, ν(C═C); 1568, ν(CN).

The water content of compounds **2**, **3** and **4** was determined by TG analysis and matches well with that obtained from elemental analysis.

Physical measurements

Elemental analyses were carried out at the "Centro de Instrumentación Científica" (University of Granada) on a Fisons-Carlo Erba analyser model EA 1108. The IR spectra on powdered samples were recorded with a ThermoNicolet IR200FTIR by using KBr pellets. Magnetisation and variable temperature (1.9–300 K) magnetic susceptibility measurements on polycrystalline samples were carried out with a Quantum Design SQUID MPMS XL-5 device operating at different magnetic fields. Magnetisation *vs.* applied field measurements were carried out at 2.0 K in the field range of 0–5 T. The experimental susceptibilities were corrected for the diamagnetism of the constituent atoms by using Pascal's tables. Luminescence spectra were measured on solid samples using a Varian Cary-Eclipse fluorescence spectrophotometer.

X-Ray crystallography

Single-crystal data collections for **1–4** were carried out at on a Bruker Apex II area-detector diffractometer using graphite monochromated Mo-Kα (λ = 0.71073 Å) radiation with the generator working at 50 kV and 30 mA. Empirical absorption corrections were applied (SADABS).[6] The structures were solved by direct methods and refined on F^2 by the SHELXL97 program.[7] Hydrogen atoms bonded to water molecules could not be reliably positioned, but the remainder of the hydrogen atoms were treated as riding atoms using the SHELX97 default parameters. It should be noted that crystals of **2** and **3** undergo a very fast degradation when they are removed from the mother liquor which has a high impact on the quality of the data. Several crystals of compounds **2** and **3** were measured and the structures were solved from the best data we were able to collect. The cations are well resolved in the structures of **2** and **3** but the counteranions and solvent molecules are not. Omission of the nitrate anions and solvents molecules entirely, followed by application of a continuous solvent area model *via* the SQUEEZE program[8] led to significant improvements in the crystallographic *R* values and also in the precision of the cationic complex. Refinement

Published on 13 July 2009 on http://pubs.rsc.org | doi:10.1039/B905330A
Downloaded by University of Belgrade on 02 January 2013

 This journal is © The Royal Society of Chemistry and the Centre National de la Recherche Scientifique 2009

View Article Online

Table 1 Crystallographic data and structural refinement details for compounds **1–4**

Compound	1	2	3	4
Chemical formula	$C_{50}H_{36}Cu_2F_{12}MnN_{10}O_{10}$	$C_{54}H_{73}N_{13}Zn_2O_{26}$	$C_{54}H_{69}N_{12}Ni_2O_{25}Cl$	$C_{54}H_{74}Co_2N_{12}O_{25}$
M/g mol^{-1}	1346.91	1450.99	1439.08	1409.11
T/K	293	150	150	150
λ/Å	0.71073	0.71073	0.71073	0.71073
Crystal system	Triclinic	Hexagonal	Hexagonal	Monoclinic
Space group	$P\bar{1}$	$P6_3/m$	$P6_3/m$	$P2_1/n$
a/Å	11.248(2)	13.645(2)	13.691(2)	15.347(3)
b/Å	12.108(2)	13.645(2)	13.691(2)	22.288(5)
c/Å	12.458(2)	22.394(1)	22.130(4)	18.484(4)
α/°	72.468(2)	90	90	90
β/°	71.400(2)	90	90	90.15(3)
γ/°	63.689(2)	120	120	90
V/Å^3	1415.6(2)	3610.8(4)	3592.5(1)	6322(2)
Z	1	2	2	4
D_c/g cm^{-3}	1.580	1.335	1.330	1.480
μ/mm^{-1}	1.068	0.747	0.642	0.616
GOF on F^2	1.045	1.119	1.108	1.164
R_1 [$I > 2\sigma(I)$]	0.069	0.061	0.048	0.070
wR_2 [$I > 2\sigma(I)$]	0.194	0.189	0.164	0.165

Published on 13 July 2009 on http://pubs.rsc.org | doi:10.1039/B905330A
Downloaded by University of Belgrade on 02 January 2013

reduced $R1$ to 0.078 and 0.045, for **2** and **3**, respectively. A summary of the crystallographic data and structure refinements are given in Table 1.

Atomic force microscopy (TMAFM)

In order to optimise the observation of the conformational changes in the tertiary structure of pBR322 DNA plasmid, it was heated at 60 °C for 30 min to obtain a majority of open circular form. 15 ng of pBR322 DNA was incubated in an appropriate volume with the required compound concentration corresponding to the molar ratio $r_i = 0.5$. The amount of compound added is expressed as r_i, and it is calculated as:

$$r_i = mN_{nucl}n/CM_rV$$

where m = the weight of the complex, M_{nucl} = the average weight per nucleotide, n = number of metal atoms in the complex, C = final concentration of DNA, M_r = molecular weight of the complex and V = final volume of the sample.

All compounds were dissolved in HEPES. The different solutions as well as Milli-Q water were passed through 0.2 μm FP030/3 filters (Schleicher & Schuell GmbH, Germany). Incubations were carried out at 37 °C for 24 h. Samples were prepared by placing a drop of DNA solution or DNA–compound solution onto peeled green mica (TED PELLA, INC., California, USA) without previous treatment. After adsorption for 5 min at room temperature, the samples were rinsed for 10 s in a jet of de-ionised water of 18 M Ω cm^{-1} from a Milli-Q water purification system directed onto the surface. The samples were blow-dried with compressed argon and then imaged by AFM.

The samples were imaged by a Nanoscope III Multimode AFM (Digital Instrumentals Inc., Santa Barbara, CA) operating in tapping mode in air at a scan rate of 1–3 Hz. The AFM probe was a 125 mm-long monocrystalline silicon cantilever with integrated conical shaped Si tips (Nanosensors GmbH, Germany) with an average resonance frequency f_o = 330 kHz and spring constant K = 50 N m^{-1}. The cantilever is rectangular and the tip radius given by the supplier is 10 nm, with a cone angle of 35° and high aspect ratio. In general the images were obtained at room temperature ($T = 23 \pm 2$ °C) and the relative humidity was usually lower than 40%.

Computational details

All DFT calculations were performed from the experimental crystallographic structures using the B3LYP functional[9] implemented in the Gaussian 03 program.[10] A quadratic convergence method was employed in the SCF process.[11] The triple-ζ quality basis set proposed by Ahlrichs and co-workers has been used for all atoms.[12] The electronic configurations used as starting points were created using the Jaguar 6.0 program.[13] More details about the use of the broken-symmetry approach to evaluate the magnetic coupling constants can be found in the literature.[14] Finally, the atomic spin densities were obtained from Natural Bond Orbital (NBO) analysis.[15]

Results and discussion

The tailored bisbidentate ligand H_2mbpb reacted in a MeOH–water mixture with $Cu(OAc)_2{\cdot}H_2O$ to afford the complex $[Cu_2(mbpb)_2]{\cdot}2H_2O$ as a black powder. Its assembly with $[Mn(hfac)_2(H_2O)_2]$ in CH_3Cl led to a green precipitate, which was further recrystallised in acetonitrile to give rise to the salt $[Mn(hfac)_2(H_2O)_2][Cu_2(mbpb)_2(CH_3CN)_2]$ (**1**). Reaction of H_2mbpb with NaOH and metal ions that have a high preference for an octahedral geometry (using a 3 : 6 : 2 molar ratio) in methanol led to dinuclear triple stranded cationic complexes $[M_2(Hmbpb)_3]X{\cdot}nH_2O$ (M = Zn^{II}, X = NO_3^- (**2**); M = Ni^{II}, X = ClO_4^- (**3**)), and the neutral species $[Co_2(mbpb)_3]{\cdot}19H_2O$ (**4**). It should be noted that Co^{II} was oxidized to Co^{III} in the course of the formation of (**4**). This process was favoured by the high ligand-field created by the fully deprotonated ligand.

Published on 13 July 2009 on http://pubs.rsc.org | doi:10.1039/B905330A
Downloaded by University of Belgrade on 02 January 2013

Crystal structures

The structure of **1** consists of neutral centrosymmetric metallamacrocycle dinuclear molecules $[Cu_2(mbpb)_2(CH_3CN)_2]$ and centrosymmetric molecules $[Mn(hfac)_2(H_2O)_2]$, which are connected by hydrogen bonds to afford a 1D system. A perspective view of the structure is given in Fig. 1, whereas relevant bond lengths and angles are gathered on Table 2.

The dinuclear molecules (see Fig. 1) exhibit a box-like achiral (C, A)[16] structure, also called *meso*-helicate or mesocate, in which the two ligands are side-by-side rather than twisted around the copper(II) ions. The $mbpb^{2-}$ bridging ligands act in a fully deprotonated bisbidentate fashion and coordinate the copper(II) ions through the pyridine and amidato nitrogen atoms with Cu–N distances of about 2 Å. This results in a twelve-membered metallamacrocyclic ring with an internal cavity of 7.423 × 3.192 Å. The copper(II) ions exhibit a distorted square-pyramidal CuN_5 five-coordination environment with $\tau = 0.28$ ($\tau = 1$ for an ideal trigonal bipyramidal geometry, D_{3h} and $\tau = 0$ for an ideal square-pyramidal geometry, C_{4v})[17] which is formed by the additional coordination of an acetonitrile molecule. In this description, one of the pyridine nitrogen atoms occupies the axial position. The ligand exhibits a non-planar conformation, with dihedral angles between the benzene and pyridine rings mean planes of 40.27 and 70.68°. The *m*-phenylene rings are strictly parallel to each other and mutually shifted, thus preventing any π···π interaction between the rings, which adopt an *anti* conformation with respect to their respective orientation into the mesocate. The intradinuclear Cu···Cu distance is 7.424 Å, whereas the shortest Cu···Cu interdinuclear distance is 7.428 Å. The general features of the structure are similar to those found in the dinuclear complex $[Cu_2L_2]$ (L = 1,3-bis(acetylacetonecarboxamide)benzene).[3g]

The Mn^{II} atoms exhibit a distorted octahedral MnO_6 coordination environment, the shortest bond distances being those connecting the Mn ion and the water oxygen atoms in *trans* positions. Strong hydrogen bonds are formed between the oxygen atoms of the water molecules coordinated to the Mn^{II} atoms and the oxygen atoms of the amidate groups with donor–acceptor distances of 2.685 and 2.765 Å, ultimately affording a chain along the [1 0 1] direction (Fig. 2).

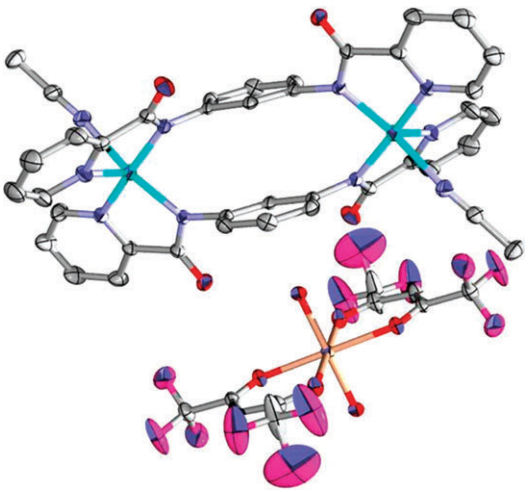

Fig. 1 Perspective view of the structure of **1**; copper (light blue), manganese (orange), oxygen (red), fluorine (pink) and nitrogen (blue). Thermal ellipsoids are drawn at the 50% probability level.

Table 2 Selected distances (Å)

Compound	**1**	**2**	**3**	**4**
$M–N_{py}$	2.004(4)	2.218(6)	2.111(1)	1.942(5)
	2.132(4)	—	—	1.945(5)
	—	—	—	1.949(4)
$M–N_{amide}$	1.959(3)	2.106(5)	2.086(1)	1.954(4)
	1.986(4)	—	—	1.960(4)
	—	—	—	1.961(4)
$M–N_{CH_3CN}$	2.212(4)	—	—	—
$M\cdots M^a$	7.424(5)	6.797(2)	6.934(1)	6.848(3)

[a] Symmetry operations: $(-x, -y, 1-z)$ for **1**, $(1-x+y, 1-x, 1/2-z)$ for **2** and **3**, Co1 and Co2 for **4**.

The structure of **2** is made of triple stranded metallocryptand cations $[Zn_2(Hmbpb)_3]^+$ (Fig. 3), nitrate anions and crystallisation water molecules. Selected bond lengths and angles are given in Table 2.

The $[Zn_2(Hmbpb)_3]^+$ cations display C_{3h} symmetry, the three-fold axis lying on the line connecting the two Zn(II) atoms, and the plane of symmetry passing through the half of the central benzene rings. Within the $[Zn_2(Hmbpb)_3]^+$ cations, symmetrically related Zn(II) atoms exhibit a ZnN_6 coordination environment with trigonally distorted octahedral geometry, which is formed by the coordination in a *fac* disposition of three amidato and three pyridine nitrogen atoms belonging to three different semideprotonated $Hmbpb^-$ bisbidentate bridging ligands. The $Zn–N_{amid}$ and $Zn–N_{py}$ bond distances are 2.218(6) and 2.106(5) Å, respectively, whereas *trans*-N–Zn–N angles are 164.5(2)° and *cis*-N–Zn–N bond angles are in the range 75.9(2)–100.6(2)°. The two octahedral ZnN_6 coordination environments exhibit opposite chirality (Δ, Λ) and consequently the $[Zn_2(Hmbpb)_3]^+$ matallocryptand cation is of the *meso*-helicate type. Hmbpb ligands exhibit a non-planar conformation, the dihedral angle between the benzene and pyridine ring being 80.87°. The benzene rings are face-to-edge π stacked with those on the adjacent ligand strands, leading to C–H···π interactions, which are responsible of the upfield shift of the C_2–H signal in the ^1H NMR spectrum of the complex ($\delta = 4.15$ ppm, see Fig. 4) with respect to the position of the same signal in the spectrum of the free ligand ($\delta = 8.53$ ppm). This upfield shift is characteristic of a proton experiencing a ring current shielding due to edge-to-face interactions.[18] The intradinuclear Zn···Zn distance is 6.797 Å whereas the shortest interdinuclear Zn···Zn distance is 9.022 Å.

The emission spectra of the H_2mbpb ligand and complex **2** in the solid state at room temperature are shown in Fig. 5. When excited at 300 nm, the ligand exhibits a fluorescence band at 450 nm. The position of this band agrees with those found in previously studied species containing pyrimidylcarboxamide groups.[19]

For **2**, the fluorescence is reduced in intensity by about 80% and remains almost at the same wavelength. Therefore, the emission is assigned to intraligand fluorescence emission (IL). While a decrease in intensity of the fluorescence emission after coordination of the ligand has been observed for many other complexes,[1g,19] in this case the increase of the conformational

 This journal is © The Royal Society of Chemistry and the Centre National de la Recherche Scientifique 2009

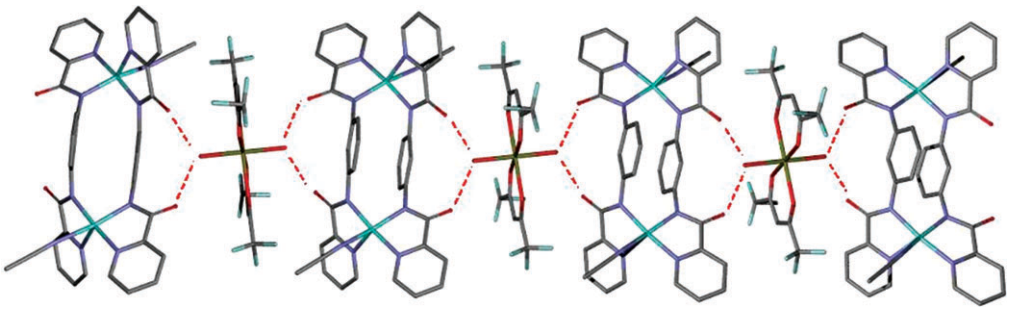

Fig. 2 Perspective view of the 1D structure of **1**; copper (light blue), manganese (yellow), oxygen (red), nitrogen (blue).

Published on 13 July 2009 on http://pubs.rsc.org | doi:10.1039/B905330A
Downloaded by University of Belgrade on 02 January 2013

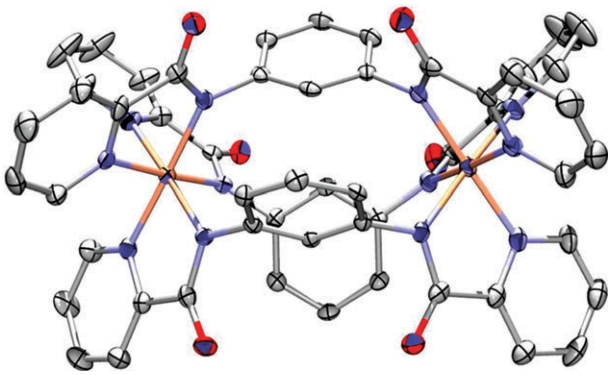

Fig. 3 Dinuclear structure of the $[Zn_2(Hmbpb)_3]^+$ cation of **2**; zinc (orange), oxygen (red), nitrogen (blue), carbon (grey). Thermal ellipsoids are drawn at the 50% probability level.

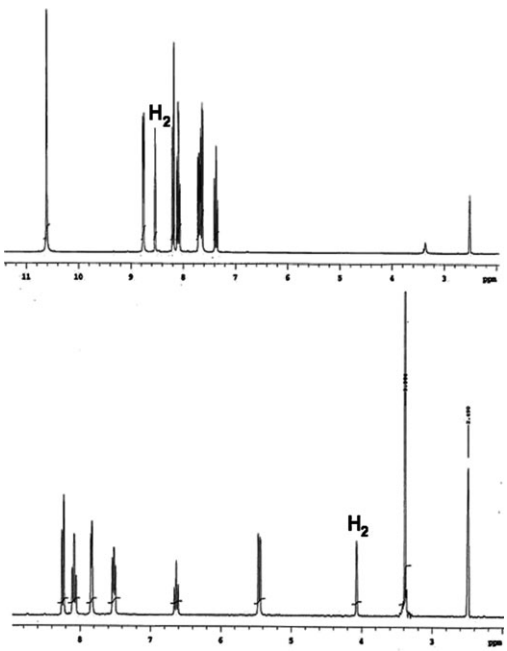

Fig. 4 ^{1}H NMR spectrum of the H_2mbpb ligand (top) and complex **2** (bottom).

rigidity of the ligands after coordination to Zn(II) should lead to an increase in intensity and not to the observed decrease (the increased rigidity should give rise to a reduction in the

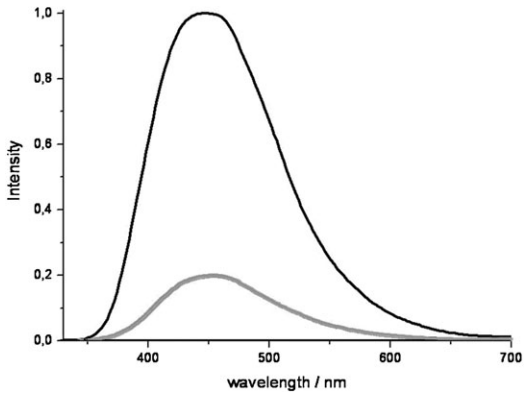

Fig. 5 Luminiscence spectra of the ligand (black) and **2** (grey) in the solid state at room temperature.

non-radiative decay of the intraligand excited state). In general, the IL emission wavelength is determined by energy gap between π and π* molecular orbitals of the free ligand, which is related to the extent of π conjugation of the system. Thus, the emission of conjugated systems can be tuned by the configuration of the ligand,[20] which depends directly on the metal coordination. In the case of **2**, where the pyridine and benzene rings are almost perpendicular (less conjugation), a blue shift of the emission band would be expected with respect to its position in the coplanar ligand, as the energy gap between π and π* molecular orbitals increases. However, this effect might be balanced by the red shift promoted by the deprotonation of the ligand, ultimately leading to an emission band that remains almost at the same energy as in the ligand.

The structure of **3** is isomorphous to that of **2** and consists of triple stranded metallocryptand $[Ni_2(Hmbpb)_3]^+$ cations, ClO_4^- anions and non-coordinated water molecules. The most relevant bond lengths and angles are given on Table 2.

The structure of **4** is made of triple stranded metallocryptand neutral molecules $[Co_2(mbpb)_3]$ and nineteen water crystallisation molecules. The most relevant differences compared with **2** and **3** affecting the dinuclear metallocryptand unit are: (a) the ligand is fully deprotonated, (b) metal ions exhibit a +3 oxidation state and (c) the molecule is a *meso*-helicate with pseudo-C_{3h} symmetry. The most relevant bond lengths and angles are given in Table 2. In this case, the ^{1}H NMR spectrum of the complex shows that the C_2–H signal is upfield shifted toward a value of δ = 3.43 ppm as a consequence of the edge-to-face C–H···π interactions.

Published on 13 July 2009 on http://pubs.rsc.org | doi:10.1039/B905330A
Downloaded by University of Belgrade on 02 January 2013

Magnetic properties

The magnetic properties of **1** in the form $\chi_M T$ *vs.* T (χ_M being the magnetic susceptibility per Cu_2Mn unit) are shown in Fig. 6.

At room temperature $\chi_M T$ is equal to 5.21 $cm^3\ mol^{-1}$ K, a value which is close to the expected spin-only value for two Cu(II) ($g = 2$, $S = 1/2$) and one Mn(II) ($g = 2$, $S = 5/2$) of 5.25 $cm^3\ mol^{-1}$ K. Upon cooling $\chi_M T$ remains almost constant until 30 K and then sharply decreases to a value of 3.79 $cm^3\ mol^{-1}$ K at 2 K. To model the magnetic properties of this compound a molecular field term accounting for the intermolecular interactions between the dinuclear $[Cu_2(mbpb)_2]$ and $[Mn(hfac)_2(H_2O)]$ units was added to the Zeeman and isotropic exchange interactions. Therefore, the Hamiltonian for this system should be written as follows:

$$H = -JS_{Cu1}S_{Cu2} + g_{Ni}\beta H(S_{Cu1} + S_{Cu2}) + g_{Mn}\beta HS_{Mn} + zJ'\langle S_z\rangle S_z$$

However, our attempts failed to simulate the $\chi_M T$ *vs.* T data with the theoretical susceptibility deduced from this model as multiple solutions were obtained.

It should be noted that theoretical and experimental studies on this type of dinuclear compounds, containing *m*-phenylene bridges and copper(II) ions separated apart by 7.56 Å, indicate ferromagnetic coupling between copper(II) ions through a spin-polarisation mechanism. In order to evaluate the intradinuclear magnetic exchange coupling for **1** we have carried out DFT/B3LYP calculations. Theoretical results show that, as it was observed in previous and similar metallacycles with oxamate derivates, the ferromagnetic coupling is a consequence of a spin polarisation mechanism[4] as the π exchange pathway along the delocalised benzene ring exhibits an alternation of the sign of the spin density (Fig. 7). Moreover, the calculated J value for **1** is $+25.3\ cm^{-1}$, which is similar but larger than those observed for other *m*-phenylene bridged dinuclear copper(II) complexes.[3] In **1**, the intermolecular antiferromagnetic interactions through the hydrogen bonding network must overcome the expected intradinuclear weak ferromagnetic interaction, leading to the observed overall weak antiferromagnetic interaction. In fact, for $J_{CuCu} = +25\ cm^{-1}$, small intermolecular antiferromagnetic exchange interactions of $zJ' = -0.15\ cm^{-1}$ are enough to predominate on the shape of the $\chi_M T$ *vs.* T curve.

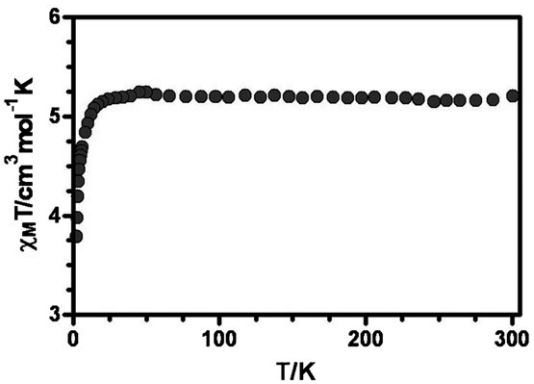

Fig. 6 $\chi_M T$ *vs.* T plot of **1** under an applied field of 0.1 T.

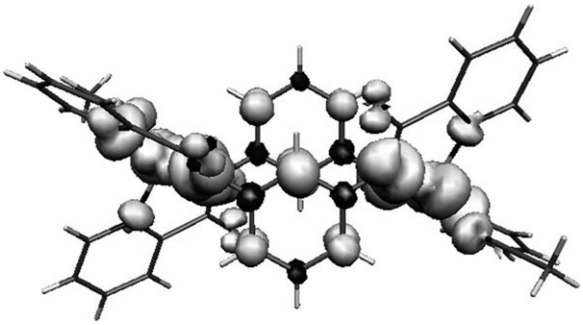

Fig. 7 Projection view of the calculated spin density distribution for the ground spin configuration of **1**. Grey and black contours represent positive and negative spin densities, respectively. The isodensity surface corresponds to a value of 0.001 e $bohr^{-3}$.

The magnetic behaviour of **3** is shown in Fig. 8 in the form of a $\chi_M T$ *vs.* T plot (χ_M being the molar susceptibility per Ni_2 unit). The value of $\chi_M T$ product at room temperature (2.30 $cm^3\ mol^{-1}$ K) matches well with that expected for uncoupled Ni(II) ions with $g = 2.15$. Upon cooling, the $\chi_M T$ product shows a continuous increase with decreasing temperature and reaches a plateau around 4 K with a value of 3.20 $cm^3\ mol^{-1}$ K, which is slightly lower than that expected for two ferromagnetically coupled Ni(II) ions with an $S = 2$ ground state (3.4 $cm^3\ mol^{-1}$ K with $g = 2.15$). The presence of this plateau points out that the zero-field splitting (ZFS) of the ground quintuplet state and the intermolecular interactions are both negligible.

As expected the isothermal magnetisation curve is well fitted by the Brillouin function for an isolated quintuplet state with $g = 2.1$. In order to simulate the experimental magnetic data, the following spin Hamiltonian was used

$$H = -JS_{Ni1}S_{Ni2} + D_{Ni}(S^2_{Ni1z} + S^2_{Ni2z}) + g\beta H(S_{Ni1} + S_{Ni2})$$

where J is the intradimer Ni(II)–Ni(II) magnetic interaction, D_{Ni} is the ZFS parameter of a single Ni(II) ion and S_{Niz} the z component of the S_{Ni} operator. The magnetic susceptibility was calculated using the MAGPACK[21] program and treating the interdimer interactions (J') in the frame of the mean-field

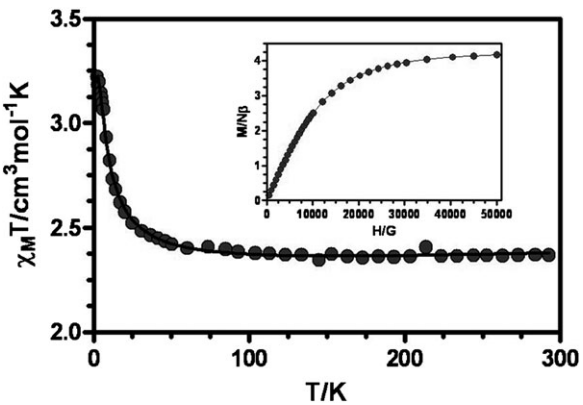

Fig. 8 Plot of $\chi_M T$ *vs.* T for **3** at 0.5 T. The solid line represents the calculated curve fit. The inset shows the field dependence of the magnetisation for **3** at 2 K (the solid line represents the Brillouin function for $S = 2$).

 This journal is © The Royal Society of Chemistry and the Centre National de la Recherche Scientifique 2009

View Article Online

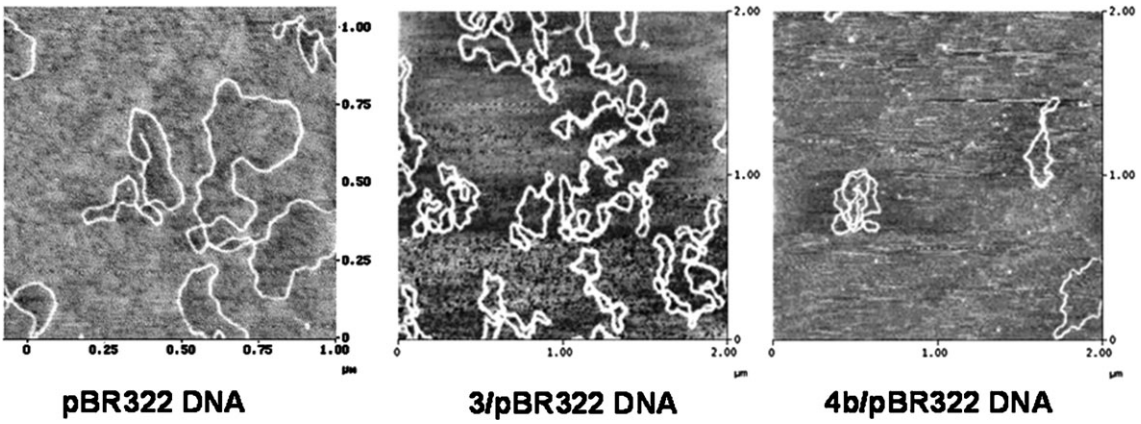

Fig. 9 AFM images of pBR322 DNA and pBR322DNA incubated for 3 h at room temperature with complexes **2** and **3**: (a) free DNA; (b) DNA incubated with the zinc complex at $r_i = 0.5$; (c) DNA incubated with the nickel complex at $r_i = 0.5$.

Published on 13 July 2009 on http://pubs.rsc.org | doi:10.1039/B905330A
Downloaded by University of Belgrade on 02 January 2013

approximation. The best set of parameters found were: $J = 3.1(2)$ cm^{-1} and $g = 2.115(8)$, $D_{Ni} = -0.4(4)$ and $zJ' = -0.077(8)$ cm^{-1}. The J value is within the range of values found for other dinuclear Ni(II) complexes with *m*-phenylene-bis(oxamato) ligands (3.1–3.6 cm^{-1}).[4f] The moderate ferromagnetic coupling is due to the spin polarisation mechanism.

DNA interaction

The DNA interaction with the complexes has been studied by atomic force microscopy (AFM) and the results are given in Fig. 9. The experiments were repeated using different samples at the same conditions of temperature and molar ratio complex : DNA, and the results obtained were always identical to those shown in Fig. 9. In all cases, the complexes seem to modify the morphology of the pBR322 DNA producing supercoiled forms in higher extension as well as kinks and cross linking. These changes might be due to interactions of the ligands with DNA through non-covalent forces.[22] Formation of covalent bonds between N sites of bases and metal ions may be discarded in this case. However, a difference appears when the effect of the Zn complex is compared with the effect of the Ni complex: the Zn complex allows the attachment of higher number of DNA forms on the mica surface while in the image corresponding to the Ni complex only a few DNA forms are attached. In light of the structural similarity of **2** and **3**, their different interaction mode with DNA may be mainly ascribed to the nature of their respective metal ions. At first glance, the only difference found between them is related with their magnetic properties. In this sense, whilst complex **3** is a paramagnetic molecule whereby two nickel(II) ions experience a weak ferromagnetic coupling, the Zn(II)-based complex **2** is diamagnetic. Nevertheless, at this stage we can not preclude other factors operating in the different behaviour of **2** and **3** with DNA, such as the relative strength of the metal–ligand interactions, their relative thermodynamic stability or their different reactivity patterns. In this connection, further investigations are being pursued extensively in our laboratory in order to shed light on the interaction of this type of mesocate complexes with DNA.

Conclusions

The tailored ligand H_2mbpb (1,3-bis(pyridine-2-carboxamide)-benzene) is able to form double stranded Cu^{II}_2 and triple stranded Ni^{II}_2, Zn^{II}_2 and Co^{III}_2 metallacyclic complexes. In the triple stranded complexes, which contain either semi-deprotonated or fully deprotonated H_2mbpb ligands, the benzene rings are face-to-edge π stacked with those on the adjacent ligand strands, leading to C–H···π interactions, which are responsible of the strong upfield shift of the C_2–H signal in the ^{1}H NMR spectra of the Zn^{II}_2 and Co^{III}_2 complexes. The Ni_2 complex exhibits ferromagnetic coupling between the metal ions through the mbpb^{2-} bridging ligand, which is due to a spin polarisation mechanism. DFT calculations have been carried out to theoretically determine the magnetic exchange coupling inside the dinuclear unit of **1**. As expected, the copper(II) ions are ferromagnetically coupled with $J = +25.3$ cm^{-1}.

Finally, the Zn^{II}_2 and Ni^{II}_2 cationic complexes interact with pBR322 DNA producing supercoiled forms in higher extension as well as kinks and cross linking. This might be due to non-covalent interactions between DNA and ligands of mesocate complexes. Interestingly, the diamagnetic Zn^{II}_2 complex allows the attachment of a higher number of DNA forms on the mica surface than the Ni^{II}_2 complex.

Acknowledgements

This work was supported by the MEC (Spain) (Projects CTQ2005/0935 and CTQ2005-08123-C02-02/BQU), the Junta de Andalucía (FQM-195), the University of Granada (grant to Antonio J. Mota and A. Rodríguez-Diéguez). M. A. P thanks to the Ministerio de Ciencia e Innovación of Spain for a FPI grant. We would like to thank the Centro de Supercomputación de la Universidad de Granada and the IQTC (Barcelona) for the computation facilities.

Notes and references

1 (*a*) C. Piguet, G. Bernardinelli and G. Hopfgartner, *Chem. Rev.*, 1997, **97**, 2005; (*b*) E. C. Constable, Polynuclear Transition Metal Helicates, in *Comprehensive Supramolecular Chemistry*, ed. J.-P. Sauvage, Elsevier, Oxford, 1996, vol. 9, p. 213; (*c*) M. Albrecht,

View Article Online

Published on 13 July 2009 on http://pubs.rsc.org | doi:10.1039/B905330A
Downloaded by University of Belgrade on 02 January 2013

Chem. Rev., 2001, **101**, 3457; (*d*) M. J. Hannon and L. J. Childs, *Supramol. Chem.*, 2004, **16**, 7; (*e*) A. F. Williams, *Chimia*, 2000, **54**, 585; (*f*) C. Piguet, M. Borkovec, J. Hamacek and K. Zeckert, *Coord. Chem. Rev.*, 2005, **101**, 3457; (*g*) N. K. Al-Rasbi, H. Adams, L. P. Harding and M. D. Ward, *Eur. J. Inorg. Chem.*, 4770, 2007, and references therein.

2 A. Oleksi, A. G. Blanco, R. Boer, I. Uson, J. Aymami, A. Rodger, M. J. Hannon and M. Coll, *Angew. Chem., Int. Ed.*, 2006, **45**, 1227.

3 S. G. Telfer, B. Bocquet and A. F. Williams, *Inorg. Chem.*, 2001, **40**, 4818.

4 (*a*) I. Fernandez, R. Ruiz, J. Faus, M. Julve, F. Lloret, J. Cano, X. Ottenwaelder, Y. Journaux and M. C. Muñoz, *Angew. Chem., Int. Ed.*, 2001, **40**, 3039; (*b*) E. Pardo, J. Faus, F. Lloret, M. C. Muñoz, J. Cano, X. Ottenwaelder, Y. Journaux, R. Carrasco, G. Blay, I. Fernández and R. Ruiz-García, *J. Am. Chem. Soc.*, 2003, **125**, 10770; (*c*) E. Pardo, K. Bernot, M. Julve, F. Lloret, J. Cano, R. Ruiz-García, J. Pasán, C. Ruiz-Pérez, X. Ottenwaelder and Y. Journaux, *Chem. Commun.*, 2004, 920; (*d*) E. Pardo, K. Bernot, M. Julve, F. Lloret, J. Cano, R. Ruiz-García and F. S. Delgado, *Inorg. Chem.*, 2004, **43**, 2768; C. Ruiz-Pérez, X. Ottenwaelder and Y. Journaux, *Chem. Commun.*, 2004, 920; (*e*) X. Ottenwaelder, J. Cano, Y. Journaux, E. Riviere, C. Brennan, M. Nierlich and R. Ruiz-Garcia, *Angew. Chem., Int. Ed.*, 2004, **43**, 850; (*f*) E. Pardo, I. Morales-Osorio, M. Julve, F. Lloret, J. Cano, R. Ruiz-García, J. Pasán, C. Ruiz-Pérez, X. Ottenwaelder and Y. Journaux, *Inorg. Chem.*, 2004, **43**, 7594; (*g*) A. R. Paital, T. Mitra, D. Ray, W. T. Wong, J. Ribas-Ariño, J. J. Novoa, J. Ribas and G. Aromí, *Chem. Commun.*, 2005, 5172; (*h*) E. Pardo, R. Ruiz-García, F. Lloret, M. Julve, J. Cano, J. Pasán, C. Ruiz-Pérez, Y. Filali, L.-M. Chamoreau and Y. Journaux, *Inorg. Chem.*, 2007, **46**, 4504; (*i*) A. R. Paital, A.-Q. Wu, G.-C. Guo, G. Aromí, J. Ribas-Ariño and D. Ray, *Inorg. Chem.*, 2007, **46**, 2947; (*j*) E. Pardo, R. Carrasco, R. Ruiz-García, M. Julve, F. Lloret, M. C. Muñoz, Y. Journaux, E. Ruiz and J. Cano, *J. Am. Chem. Soc.*, 2008, **130**, 576; (*k*) E. Pardo, R. Ruiz-García, J. Cano, X. Ottenwaelder, R. Lescouëzec, Y. Journaux, F. Lloret and M. Julve, *Dalton Trans.*, 2008, 2780; (*l*) D. Cangussu, E. Pardo, M.-C. Dul, R. Lescouëzec, P. Herson, Y. Journaux, E. F. Pedrosa, C. L. M. Pereira, H. O. Stumpf, M. C. Muñoz, R. Ruiz-García, J. Cano, M. Julve and F. Lloret, *Inorg. Chim. Acta*, 2008, **361**, 3394.

5 M. Ray, R. Mukherjee, J. F. Richardson and R. M. Buchanan, *J. Chem. Soc., Dalton Trans.*, 1993, 2451.

6 G. M. Sheldrick, *SADABS, Program for Area Detector Adsorption Correction*, Institute for Inorganic Chemistry, University of Göttingen, Germany, 1996.

7 G. M. Sheldrick, *SHELX 97*, University of Göttingen, Göttingen, Germany, 1997.

8 A. L. Spek, PLATON-94 (V-101094). *A Multipurpose Crystallographic Tool*, University of Utrecht, The Netherlands, 1994.

9 A. D. Becke, *Phys. Rev. A*, 1988, **38**, 3098; C. T. Lee, W. T. Yang and R. G. Parr, *Phys. Rev. B*, 1988, **37**, 785; A. D. Becke, *J. Chem. Phys.*, 1993, **98**, 5648.

10 M. J. Frisch, G. W. Trucks, H. B. Schlegel, G. E. Scuseria, M. A. Robb, J. R. Cheeseman, J. A. Montgomery, Jr., T. Vreven, K. N. Kudin, J. C. Burant, J. M. Millam, S. S. Iyengar, J. Tomasi, V. Barone, B. Mennucci, M. Cossi, G. Scalmani, N. Rega, G. A. Petersson, H. Nakatsuji, M. Hada, M. Ehara, K. Toyota, R. Fukuda, J. Hasegawa, M. Ishida, T. Nakajima, Y. Honda, O. Kitao, H. Nakai, M. Klene, X. Li, J. E. Knox, H. P. Hratchian, J. B. Cross, V. Bakken, C. Adamo, J. Jaramillo, R. Gomperts, R. E. Stratmann, O. Yazyev, A. J. Austin, R. Cammi, C. Pomelli, J. Ochterski, P. Y. Ayala, K. Morokuma, G. A. Voth, P. Salvador, J. J. Dannenberg, V. G. Zakrzewski, S. Dapprich, A. D. Daniels, M. C. Strain, O. Farkas, D. K. Malick, A. D. Rabuck, K. Raghavachari, J. B. Foresman, J. V. Ortiz, Q. Cui, A. G. Baboul, S. Clifford, J. Cioslowski, B. B. Stefanov, G. Liu, A. Liashenko, P. Piskorz, I. Komaromi, R. L. Martin, D. J. Fox, T. Keith, M. A. Al-Laham, C. Y. Peng, A. Nanayakkara, M. Challacombe, P. M. W. Gill, B. G. Johnson, W. Chen, M. W. Wong, C. Gonzalez and J. A. Pople, *GAUSSIAN03 (Revision C.2)*, Gaussian, Inc., Wallingford, CT, 2004.

11 G. B. Bacskay, *Chem. Phys.*, 1981, **61**, 385.

12 (*a*) A. Schafer, H. Horn and R. Ahlrichs, *J. Chem. Phys.*, 1992, **97**, 2571; (*b*) A. Schaefer, C. Huber and R. Ahlrichs, *J. Chem. Phys.*, 1994, **100**, 5829.

13 *Jaguar 6.0*, Schrödinger, Inc., Portland, 2005.

14 (*a*) E. Ruiz, P. Alemany, S. Alvarez and J. Cano, *J. Am. Chem. Soc.*, 1997, **119**, 1297; (*b*) E. Ruiz, J. Cano, S. Alvarez and P. Alemany, *J. Comput. Chem.*, 1999, **20**, 1391; (*c*) E. Ruiz, A. Rodríguez-Fortea, J. Cano, S. Alvarez and P. Alemany, *J. Comput. Chem.*, 2003, **24**, 982; (*d*) E. Ruiz, S. Alvarez, J. Cano and V. Polo, *J. Chem. Phys.*, 2005, **123**, 164110.

15 (*a*) J. E. Carpenter and F. Weinhold, *J. Mol. Struct.*, 1988, **169**, 41; (*b*) A. E. Reed, L. A. Curtis and F. Weinhold, *Chem. Rev.*, 1988, **88**, 899; (*c*) F. Weinhold, J. E. Carpenter, *The Structure of Small Molecules and Ions*, Plenum, New York, 1988, p. 227.

16 N. G. Conelly, T. Damhus, R. M. Hartshorn and A. T. Hutton, *Nomenclature of Inorganic Compounds. IUPAC Recommendations*, Royal Society of Chemistry, Cambridge, UK, 2005.

17 A. W. Addison, T. N. Rao, J. Reedijk, J. van Rijn and G. C. Verschoor, *J. Chem. Soc., Dalton Trans.*, 1984, 1349.

18 W. B. Jennings, B. M. Farrell and J. F. Malone, *J. Org. Chem.*, 2006, **71**, 2277.

19 B.-L. Wu, P. Zhang, Y.-Y. Niu, H.-Y. Zhang, Z.-J. Li and H.-W. Hou, *Inorg. Chim. Acta*, 2008, **361**, 2203, and references therein.

20 (*a*) S. Aoki, D. KAgata, M. Shiro, K. Takeda and E. Kimura, *J. Am. Chem. Soc.*, 2004, **126**, 13377; (*b*) B. Wu, D. Yuan, F. Jiang, R. Wang, L. Han, Y. Zhou and M. Hong, *Eur. J. Inorg. Chem.*, 2004, 2695.

21 (*a*) J. J. Borrás-Almenar, J. Clemente, E. Coronado and B. S. Tsukerblat, *Inorg. Chem.*, 1999, **38**, 6081; (*b*) J. J. Borrás-Almenar, J. Clemente, E. Coronado and B. S. Tsukerblat, *J. Comput. Chem.*, 2001, **22**, 985.

22 C. Uerpmann, J. Malina; M. Pascu, G. J. Clarkson, V. Moreno, A. Rodger, A. Grandas and M. J. Hannon, *Chem.–Eur. J.*, 2005, **11**, 1750–1756.

 This journal is © The Royal Society of Chemistry and the Centre National de la Recherche Scientifique 2009